

# Axisymmetric Steady Solutions in an Idealized Model of Atmospheric General Circulations: Hadley Circulation and Super-rotation

Hiroki YAMAMOTO\*, Keiichi ISHIOKA\* and Shigeo YODEN\*

*\*Graduate School of Science, Kyoto University, Kyoto*

Fundamental dynamics of two-dimensional atmospheric general circulations symmetric about the rotation axis of planets is investigated to obtain a wide perspective from the Held and Hou model of the Hadley circulation to the Venus-like super-rotation driven by the Gierasch mechanism. A parameter sweep experiment is performed to explore steady solutions of the axisymmetric primitive equations of the Boussinesq fluid on a rotating sphere. Sweep parameters are the external thermal Rossby number ( $R_T$ ), the horizontal Ekman number ( $E_H$ ), and the vertical Ekman number ( $E_V$ ). Two indices are introduced to make a dynamical analysis of the numerically obtained circulations: a measure of the intensity of super-rotation ( $S$ ) and a measure of rigid rotation ( $Rg$ ). The characteristics of steady solutions change largely in a certain range of  $E_H$  for given  $R_T$  and  $E_V$ . Approximate positions of this transition can be estimated theoretically as  $E_H \sim E_V S(R_T)$ , where  $S \sim R_T$  for  $R_T \leq 1$  and  $S \sim \sqrt{R_T}$  for  $R_T > 1$ .

## 1. INTRODUCTION

The Hadley circulation is an important part of the general circulation of the atmosphere. Schneider (1977)<sup>1)</sup> and Held and Hou (1980<sup>2)</sup>, HH80 hereafter) studied the Hadley circulation by using an idealized two-dimensional numerical model symmetric with respect to the rotation axis of the Earth with no horizontal eddy diffusion. HH80 explained the basic dynamics of the Hadley circulation with a few physical principles: (i) the polewards moving air conserves its axial angular momentum, whereas the zonal flow associated with the near-surface, equatorwards moving flow is frictionally retarded and is weak; (ii) the circulation is in thermal wind balance (Vallis, 2006<sup>3)</sup>). This is known as the Held and Hou (HH hereafter) model. After this theory, a lot of studies applying the HH model were carried out; see Lindzen (1990)<sup>4)</sup>, James (1994)<sup>5)</sup>, Satoh (1994)<sup>6)</sup>, Williams (2003)<sup>7)</sup> and their references.

Super-rotation, a state of an atmosphere rotating much faster than the planet, is one of the prominent phenomena observed in the Venus and the Titan, which is the largest moon of the Saturn. Gierasch (1975)<sup>8)</sup> studied the mechanism of the super-rotation assuming an axial symmetric circulation and an infinitely large horizontal eddy diffusion. The Gierasch mechanism was studied by Matsuda (1980<sup>9)</sup>, 1982<sup>10)</sup>, M80/82 hereafter) using a model of Boussinesq fluid with a finitely large horizontal eddy diffusion.

Actually, both HH80 and M80/82 used the same system: the primitive equations of Boussinesq fluid with a Newtonian heating/cooling to force the flow field, assuming a steady state, and axial and equatorial symmetries. The main differences between them are the values of the horizontal eddy diffusion coefficient ( $\nu_H$ ) and the angular velocity of the planet ( $\Omega$ ). In other words, this

system has the Hadley solution of HH type when  $\Omega$  is large (like the Earth) and  $\nu_H = 0$ ; on the other hand, when  $\Omega$  is small (like the Venus) and  $\nu_H$  is very large, the system has the super-rotation solution of Gierasch-Matsuda (GM hereafter) type: an atmosphere rotating much faster than the planet in nearly rigid rotation.

In the present study, we explore steady solutions from the HH type circulation to the GM type circulation by a parameter sweep experiment. Transition between two types of circulation and its parameter dependence are investigated by introducing a measure of the intensity of super-rotation and that of rigid rotation.

## 2. DESCRIPTIONS OF THE SYSTEM

### Governing equations

The governing equations used in this study are the primitive equations of Boussinesq fluid with a Newtonian heating/cooling, under the assumptions of a steady state ( $\partial/\partial t = 0$ , where  $t$  is time), axial symmetry ( $\partial/\partial \lambda = 0$ , where  $\lambda$  is longitude), and equatorial symmetry. The equations in spherical geometry are given by,

$$\frac{v}{a} \frac{\partial u}{\partial \phi} + w \frac{\partial u}{\partial z} - \frac{uv \tan \phi}{a} - 2\Omega v \sin \phi = \nu_H D_H(u) + \nu_V \frac{\partial^2 u}{\partial z^2}, \quad (1)$$

$$\frac{v}{a} \frac{\partial v}{\partial \phi} + w \frac{\partial v}{\partial z} + \frac{u^2 \tan \phi}{a} + 2\Omega u \sin \phi = -\frac{1}{a} \frac{\partial \Phi}{\partial \phi} + \nu_H D_H(v) + \nu_V \frac{\partial^2 v}{\partial z^2}, \quad (2)$$

$$\frac{v}{a} \frac{\partial \Theta}{\partial \phi} + w \frac{\partial \Theta}{\partial z} = -\frac{\Theta - \Theta_e}{\tau} + \kappa_V \frac{\partial^2 \Theta}{\partial z^2}, \quad (3)$$

$$\frac{\partial \Phi}{\partial z} = g\alpha\Theta, \quad (4)$$

$$\frac{1}{a \cos \phi} \frac{\partial}{\partial \phi} (v \cos \phi) + \frac{\partial w}{\partial z} = 0. \quad (5)$$

Here  $u, v, w$  are the zonal, meridional, and vertical components of the velocity,  $\Theta$  is the potential temperature, and  $\Phi \equiv p/\rho$ , where  $p$  is the pressure and  $\rho$  is the density. Independent variables  $\phi$  and  $z$  are the latitude and height, respectively. The constants  $a$  and  $\Omega$  are the radius and angular velocity of the planet,  $g$  is the gravitational acceleration,  $\tau$  is the time constant for Newtonian heating/cooling,  $\nu_H$  and  $\nu_V$  are the horizontal and vertical diffusion coefficients,  $\kappa_V$  is the vertical thermal diffusion coefficient, and  $\alpha$  is the thermal expansion coefficient.

The quantity  $\Theta_e$  in the Newtonian heating/cooling term in equation (3) is a potential temperature in radiative equilibrium which is given by the form

$$\frac{\Theta_e}{\Theta_0} = 1 - \frac{2}{3} \Delta_H P_2(\sin \phi) + \Delta_V \left( \frac{z}{H} - \frac{1}{2} \right), \quad (6)$$

where  $\Theta_0$  is the global mean of  $\Theta_e$ ,  $\Delta_H$  and  $\Delta_V$  are the fractional change of potential temperature in radiative equilibrium from equator to pole and from the top to the bottom, respectively, and  $P_2$  is the second Legendre polynomial  $P_2(x) = (3x^2 - 1)/2$ . We assume the thermal expansion coefficient as  $\alpha = 1/\Theta_0$ .

Horizontal diffusion terms,  $D_H(u)$  and  $D_H(v)$ , are defined in the form to conserve angular mo-

mentum (Becker, 2001<sup>11</sup>), as follows:

$$D_H(u) = \frac{1}{a^2 \cos \phi} \frac{\partial}{\partial \phi} \left( \cos \phi \frac{\partial u}{\partial \phi} \right) - \frac{u}{a^2 \cos^2 \phi} + \frac{2u}{a^2}, \quad (7)$$

$$D_H(v) = \frac{1}{a^2 \cos \phi} \frac{\partial}{\partial \phi} \left( \cos \phi \frac{\partial v}{\partial \phi} \right) - \frac{v}{a^2 \cos^2 \phi} + \frac{1}{a} \frac{\partial}{\partial \phi} \left[ \frac{1}{a \cos \phi} \frac{\partial}{\partial \phi} (v \cos \phi) \right] + \frac{2v}{a^2}. \quad (8)$$

A zero stress condition is imposed at the top boundary, at  $z = H$ , and the stress at the ground is taken to be proportional to the surface wind. Zero vertical heat flux is imposed at both top and bottom boundaries, so boundary conditions are

$$w = \frac{\partial u}{\partial z} = \frac{\partial v}{\partial z} = \frac{\partial \Theta}{\partial z} = 0 \quad \text{at} \quad z = H, \quad (9)$$

$$w = \frac{\partial \Theta}{\partial z} = 0, \quad \nu_V \frac{\partial u}{\partial z} = Cu, \quad \nu_V \frac{\partial v}{\partial z} = Cv \quad \text{at} \quad z = 0, \quad (10)$$

where  $C$  is a drag coefficient.

### Non-dimensionalization

To clarify the dependence of obtained solutions on the external parameters, we derive non-dimensional form of the governing equations. First, we write variables as,

$$u = Uu^*, \quad v = Vv^*, \quad w = Ww^*, \quad \Theta = \Theta_0\Theta^*, \quad \text{and} \quad z = Hz^*, \quad (11)$$

where  $U, V, W, \Theta_0$ , and  $H$  are the scaling values, and the asterisk denotes non-dimensional variables. From the hydrostatic equation (4),  $\Phi$  can be scaled as

$$\Phi = gH\Phi^*, \quad (12)$$

and from the meridional derivative of (4),  $\partial\Phi/\partial\phi$  can be scaled as

$$\frac{\partial\Phi}{\partial\phi} = \beta\Delta_H gH \frac{\partial\Phi^*}{\partial\phi}, \quad (13)$$

where  $\beta \equiv (\partial\Theta/\partial\phi)/(\partial\Theta_e/\partial\phi)$  is the ratio between meridional gradient of potential temperature and that in the radiative equilibrium state. Substituting (11), (12), and (13) to the governing equations (1)-(5), the non-dimensional equations are obtained as follows (asterisks are omitted),

$$R_v v \frac{\partial u}{\partial \phi} + R_w w \frac{\partial u}{\partial z} - R_v u v \tan \phi - \frac{2}{\gamma} v \sin \phi = E_H D_H(u) + E_V \frac{\partial^2 u}{\partial z^2}, \quad (14)$$

$$R_v v \frac{\partial v}{\partial \phi} + R_w w \frac{\partial v}{\partial z} + R_v \gamma^2 u^2 \tan \phi + 2\gamma u \sin \phi = -\beta \frac{R_T}{R_v} \frac{\partial \Phi}{\partial \phi} + E_H D_H(v) + E_V \frac{\partial^2 v}{\partial z^2}, \quad (15)$$

$$R_v v \frac{\partial \Theta}{\partial \phi} + R_w w \frac{\partial \Theta}{\partial z} = -\frac{1}{\epsilon} \left[ \Theta - 1 + \frac{2}{3} \Delta_H P_2(\sin \phi) - \Delta_V \left( z - \frac{1}{2} \right) \right] + \frac{E_V}{Pr_V} \frac{\partial^2 \Theta}{\partial z^2}, \quad (16)$$

$$\frac{\partial \Phi}{\partial z} = \Theta, \quad (17)$$

$$R_v \frac{1}{\cos \phi} \frac{\partial}{\partial \phi} (v \cos \phi) + R_w \frac{\partial w}{\partial z} = 0. \quad (18)$$

Here the non-dimensional numbers are

external thermal Rossby number:  $R_T \equiv \frac{gH\Delta_H}{a^2\Omega^2}$ ,

horizontal and vertical Ekman numbers:  $E_H \equiv \frac{\nu_H}{a^2\Omega}$  and  $E_V \equiv \frac{\nu_V}{H^2\Omega}$ ,

vertical Prandtl number:  $Pr_V \equiv \frac{\nu_V}{\kappa_V}$ ,

Rossby numbers scaled with meridional and vertical velocity:  $R_v \equiv \frac{V}{a\Omega}$  and  $R_w \equiv \frac{W}{H\Omega}$ ,

the ratio of zonal velocity to meridional velocity:  $\gamma \equiv \frac{U}{V}$ ,

and the ratio of the time constant for Newtonian heating/cooling to the period of the rotation:  $\epsilon \equiv \tau\Omega$ .

From (18), we can show  $R_v \sim R_w$  immediately. From the boundary condition (10), we obtain another non-dimensional number  $\zeta \equiv \nu_V/(C\delta z)$ , where  $\delta z$  is the height of the lowest layer.

These non-dimensional parameters consist of two groups depending on whether the value is determined externally in each experiment, or not. External parameters are  $R_T, E_H, E_V, Pr_V, \epsilon, \zeta, \Delta_H$ , and  $\Delta_V$ , while internal parameters are  $R_v, \beta$ , and  $\gamma$ . If we fix the non-dimensional external parameters, the solution of the governing equations is expected to be similar.

### 3. A PARAMETER SWEEP EXPERIMENT

A parameter sweep experiment is designed to investigate steady solutions of the system, from the HH type Hadley circulation to the GM type super-rotation. Because  $R_T, E_H$ , and  $E_V$  are key parameters of HH80 and M80/82, these are chosen for sweep parameters. Constructing a parameter space  $(R_T, E_H, E_V)$  as Fig.1, we can draw the planes which correspond to the parameter ranges of HH80 and M80/82. Our main interest is the transition of the steady solutions between two well

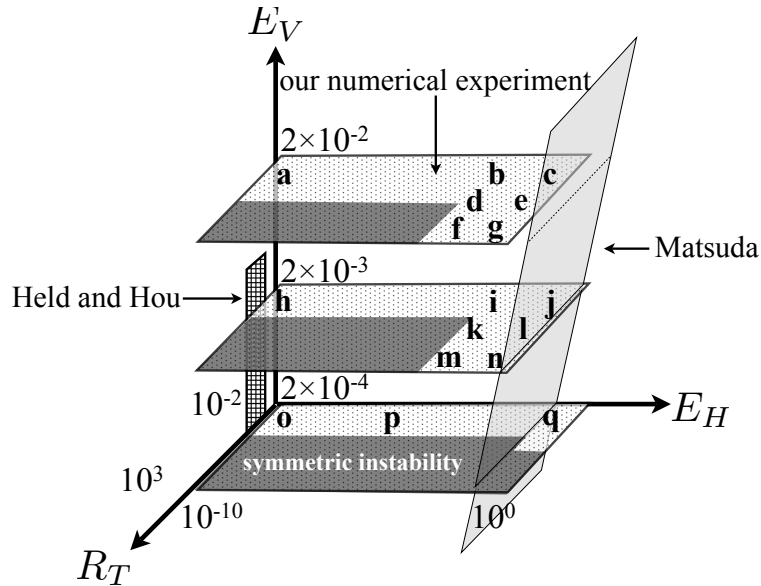


Fig. 1: Positions of Held and Hou (1980, mesh plane), Matsuda (1980, 1982, light gray plane), and our numerical experiment (dotted plane) in a parameter space  $(R_T, E_H, E_V)$ . The dark areas denote the regions where the solution fails to achieve a steady state because of a symmetric instability. Alphabet letters indicate the positions of the cases where zonal wind fields and meridional streamfunctions are shown in Fig.2 and Fig.3.

known situations. Note that the Grashof number ( $G_r$ ) which M80/82 used for a sweep parameter is related to  $R_T$  and  $E_V$  by  $G_r = R_T/E_V^2$ . Furthermore, the plane of M80/82 drawn in Fig.1 corresponds to only a part of the investigated range in M80/82.

We construct a numerical model of the time-dependent version of the governing equations (1)-(10), using a spectral transform method for meridional direction, a central difference method for vertical direction, and the 4th order Runge-Kutta method for the time-integrations. The truncation order of Legendre polynomial is 85 (64 grid points from equator to pole for the Gaussian latitudes) and the number of layers in vertical is 32. The initial condition is a state at rest with a constant potential temperature  $\Theta_0$ , and the time-integrations are done with a time step of 1 hour until a steady state is achieved.

To sweep  $R_T$ ,  $E_H$ , and  $E_V$  with other non-dimensional external parameters fixed, we change the values of  $\Omega$ ,  $\tau$ ,  $\nu_H$ ,  $\nu_V$ ,  $\kappa_V$ , and  $C$  while the other parameters are fixed as follows:  $a = 6.4 \times 10^6$  m,  $H = 8 \times 10^3$  m,  $\delta z = 250$  m,  $g = 9.8$  m/s<sup>2</sup>,  $\Theta_0 = 250$  K,  $\Delta_H = 1/3$ , and  $\Delta_V = 1/8$ . Sweeping ranges are  $1.2 \times 10^{-2} \leq R_T \leq 1.2 \times 10^3$ ,  $3.3 \times 10^{-10} \leq E_H \leq 1.3 \times 10^0$ , and  $2.1 \times 10^{-4} \leq E_V \leq 2.1 \times 10^{-2}$  as shown in Fig.1. The other non-dimensional external parameters are fixed as  $Pr_V = 1$ ,  $\epsilon = 126$ , and  $\zeta = 0.8$ .

## 4. NUMERICAL RESULTS

We execute 342 runs to obtain steady solutions numerically in the parameter range described above. However, the calculations indicated by the dark areas in Fig.1 fail to achieve a steady state. Spatial distribution of the potential vorticity indicates that symmetric instability occurs when the numerical solution does not converge to a steady state. In this study, however, we focus on the steady solutions, not on time-dependent ones.

Figures 2 and 3 show zonal wind fields and meridional streamfunctions, respectively, of steady solutions for the cases indicated by alphabet letters in Fig.1. The parameter values for the case **o** are similar to those given in HH80, and the obtained steady solution is also similar: the Hadley circulation with weak indirect Ferrel cell. The panels **p** and **q** ( $E_H = 3.3 \times 10^{-5}$ ,  $3.3 \times 10^{-1}$ ), which are for the cases of much larger  $E_H$  than **o** ( $E_H = 3.3 \times 10^{-10}$ ), show that the zonal wind field changes to a rigid rotation state, and the Hadley circulation weakens and expands to pole. Similar transition can be seen for the cases of  $E_V = 2.1 \times 10^{-3}$  (**h**, **i**, and **j**). The cases **j** and **q** correspond to the solution of thermal wind balance of the Earth type in M80/82. When  $R_T$  is increased at large  $E_H$  of  $3.3 \times 10^{-1}$ , the pattern of rigid rotation does not change very much, but the relative rotation speed of the atmosphere to the planet increases. When  $R_T = 1.2 \times 10^3$  (the case **n**), the zonal wind speed at the top boundary is about ten times faster than the rotation speed of the planet  $a\Omega$  (about 4.7 m/s). This is a typical super-rotation state, and corresponds to the solution of thermal wind balance of the Venus type in M80/82. For a large value of  $E_V = 2.1 \times 10^{-2}$ , the zonal wind speed is reduced for all parameter values of  $R_T$  and  $E_H$  because of the strong vertical diffusion as shown in the panels **a-g**.

## 5. DYNAMICAL ANALYSIS OF THE TRANSITION

For the dynamical analysis of the transition from the HH type Hadley circulation to the GM type super-rotation, we consider this transition as two parts by introducing two indices: the increase of the intensity of super-rotation and the transition of the zonal wind field to a rigid rotation state.

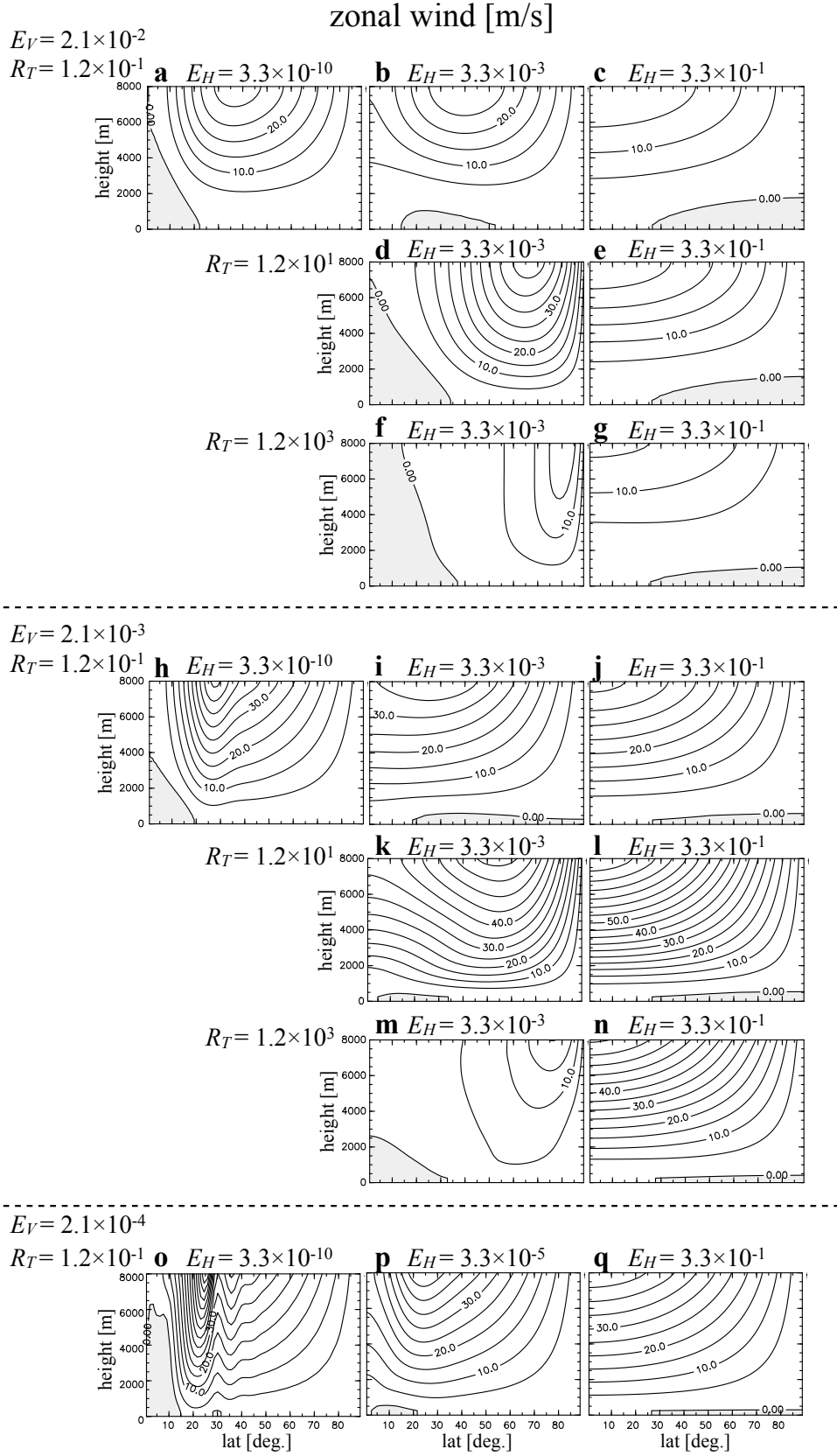


Fig. 2: Numerically obtained zonal wind fields for some combinations of external parameters  $R_T$ ,  $E_H$ , and  $E_V$ . Values of the sweep parameters are shown in the top and left of each panels. Alphabet letters on this figure correspond to those on Fig.1. Contour intervals are 5 m/s. Shade areas indicate the regions of negative values.

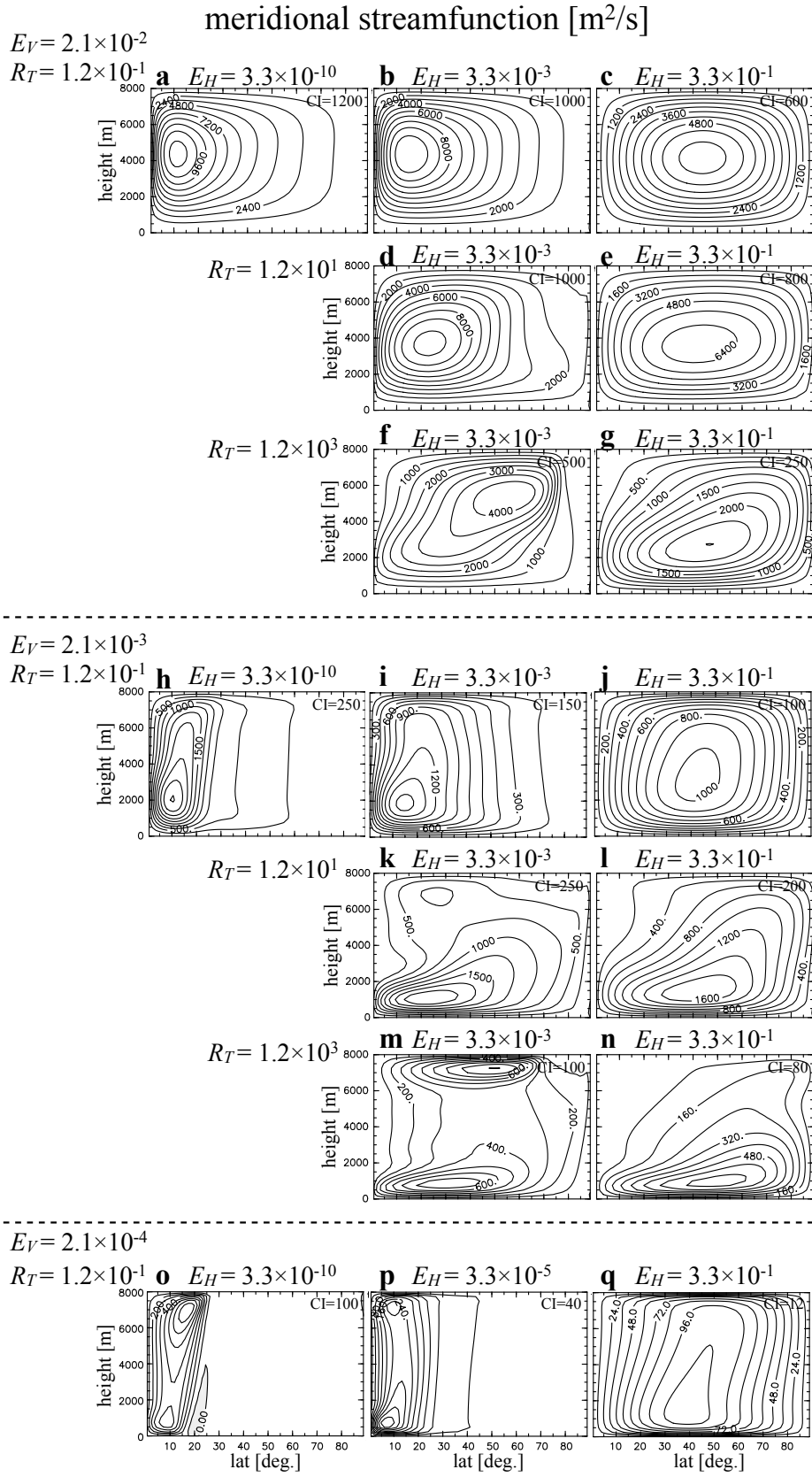


Fig. 3: Same as Fig.2, but for meridional streamfunctions. Contour intervals are shown at right top of each panels.

## Intensity of super-rotation

We introduce a measure of the intensity of super-rotation,  $S$ , which is defined as a latitudinally averaged zonal wind at the top boundary, from equator to pole, divided by the planetary rotation speed; namely  $S \equiv U/(a\Omega)$ . In this study, we call a state with  $S \geq 1$  a super-rotation state. The dependence of  $S$  on  $R_T, E_H$ , and  $E_V$  are shown in Fig.4. The value of  $S$  becomes larger than unity when both  $E_H$  and  $R_T$  are large:  $R_T \geq 4$  for  $E_H = 3.3 \times 10^{-1}$  and  $E_V = 2.1 \times 10^{-3}$ , and  $R_T \geq 60$  for  $E_H = 3.3 \times 10^{-1}$  and  $E_V = 2.1 \times 10^{-2}$ . However, when the horizontal diffusion  $E_H$  is not so large ( $E_H = 3.3 \times 10^{-3}$ ),  $S$  is less than unity, even if  $R_T$  becomes large as  $R_T = 1.2 \times 10^3$ . This diagram shows a very large horizontal diffusion is necessary for super-rotation, and a smaller vertical diffusion is preferable for that.

From a simple consideration of geostrophic balance and cyclostrophic balance, we can obtain the estimate of  $S$  as a function of  $R_T$ . If we neglect the advection terms and the diffusion terms, the equation (15) becomes

$$S^2 u^2 \tan \phi + 2Su \sin \phi \sim -R_T \frac{\partial \Phi}{\partial \phi}. \quad (19)$$

Here,  $R_v \gamma$  is approximated by  $S$ , and  $\beta$  is assumed to be unity. From equation (19),  $S$  is approximated as:

$$S \sim \begin{cases} R_T & \text{for } R_T \ll 1 : \text{geostrophic balance} \\ \sqrt{R_T} & \text{for } R_T \gg 1 : \text{cyclostrophic balance} \end{cases}. \quad (20)$$

Even when  $R_T \sim 1$ , this can be applied as:

$$S \sim \begin{cases} R_T & \text{for } R_T \leq 1 \\ \sqrt{R_T} & \text{for } R_T > 1 \end{cases}, \quad (21)$$

in Fig.4 (solid line). Equation (21) is a good estimate over a wide parametric range of  $R_T$ , when  $E_V$  is small and  $E_H$  is large. We should note that above estimation corresponds to the argument on thermal wind balance of the Earth type and the Venus type done by M80 (his equation 3.13)

## A measure of rigid rotation

The second index is a measure of rigid rotation,  $Rg$ , defined as the ratio of the rigid rotation component of the kinetic energy of the zonal wind to the zonal kinetic energy at the top boundary,

$$Rg \equiv \frac{\text{rigid rotation component of } KE \text{ of the zonal wind}}{KE \text{ of the zonal wind}} \Big|_{z=H} = \frac{2|\psi_1|^2}{\sum n(n+1)|\psi_n|^2} \Big|_{z=H}, \quad (22)$$

where  $\psi_n$  ( $n = 1, 2, \dots$ ) is a Legendre polynomial expansion coefficient of the horizontal streamfunction. Figure 5 shows the dependence of  $Rg$  on  $E_H$  for five combinations of  $R_T$  and  $E_V$ . When  $E_H$  is very large,  $Rg$  is nearly unity; namely the zonal wind field is almost rigid rotation. The zonal wind at the top boundary for the case **(vi)** in Fig.6 shows such a rigid rotation state. In contrast, when  $E_H$  is very small,  $Rg$  takes a certain constant value which depends mostly on  $R_T$ . This solution corresponds to the HH type Hadley circulation as shown by Fig.6 **(i)**. The circulation changes largely from the HH type solution to the rigid rotation state in a certain range of  $E_H$  as **(ii)**-**(v)** in Fig.5. The zonal wind increases at low latitudes in the cases for this range as shown in Fig.6.

An approximate position of the transition in Fig.5 where the circulation type changes from the HH type to rigid rotation can be estimated with the  $u$ -momentum equation (1), whose terms in left hand side are rewritten with absolute angular momentum per unit mass,  $M \equiv a^2 \Omega \cos^2 \phi + ua \cos \phi$ ,

$$\frac{1}{a \cos \phi} \nabla \cdot (\mathbf{v}M) = \nu_H D_H(u) + \nu_V \frac{\partial^2 u}{\partial z^2}, \quad (23)$$



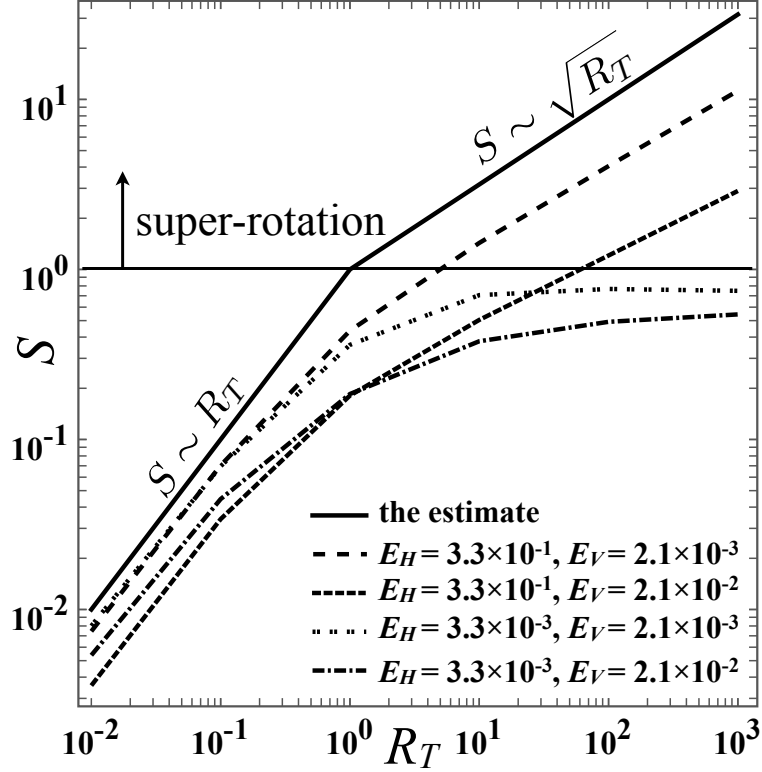


Fig. 4: The dependence of the intensity of super-rotation  $S$  on the external thermal Rossby number  $R_T$ , for some combinations of the horizontal Ekman number  $E_H$  and the vertical Ekman number  $E_V$ . The solid line represents the estimate of  $S$  under the assumption of geostrophic balance and cyclostrophic balance.

where  $\mathbf{v} \equiv (v, w)$  is the velocity, and  $\nabla \equiv [(a \cos \phi)^{-1} \partial(\cos \phi) / \partial \phi, \partial / \partial z]$  is the gradient operator in the meridional plane. When  $\nu_H$  is small enough, the balance between the flux divergence term and the vertical diffusion term is dominant for the HH type Hadley circulation. As  $\nu_H$  increase, the second term in equation (23) becomes large. It is expected that the transition takes place when the horizontal diffusion term is comparable to the vertical diffusion term. The magnitude of the horizontal diffusion term in the HH type circulation is estimated as follows. Outside the Hadley cell, zonal wind field is in a rigid rotation state as  $u_E = a\Omega[(1 + 2R_T z/H)^{1/2} - 1] \cos \phi$ , because of the thermal wind balance to the radiative equilibrium potential temperature field, and the horizontal diffusion term becomes zero. In the Hadley cell, on the other hand, zonal winds at the top boundary are determined by the angular momentum conservation as  $u_M = a\Omega \sin^2 \phi / \cos \phi$ . Therefore, the magnitude of the horizontal diffusion term in the HH type circulation is the order of  $\nu_H a \Omega / a^2$ , so the transition takes place when

$$\nu_H \frac{a\Omega}{a^2} \sim \nu_V \frac{U}{H^2}, \quad (24)$$

so that

$$E_H \sim E_V S. \quad (25)$$

The relationship (21) is used for the value of  $S$  to estimate the position of the transition with equation (25). Arrows in Fig.5 show the estimates for the combination of  $R_T$  and  $E_V$ , and these points agree well with the transitions.

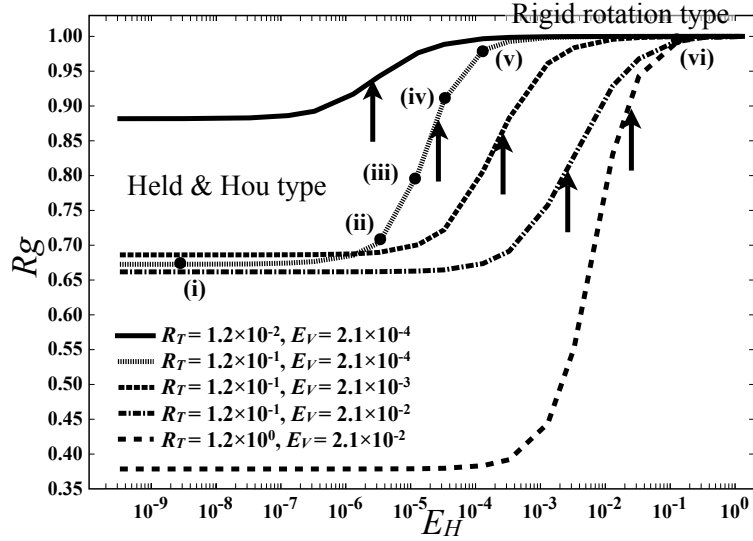


Fig. 5: The dependence of the measure of rigid rotation  $Rg$  on the horizontal Ekman number  $E_H$ , for some combinations of the external thermal Rossby number  $R_T$  and the vertical Ekman number  $E_V$ . Estimated transition points ( $E_H \sim E_V S$ ) are shown by arrows. Roman numerals correspond to those of Fig.6.

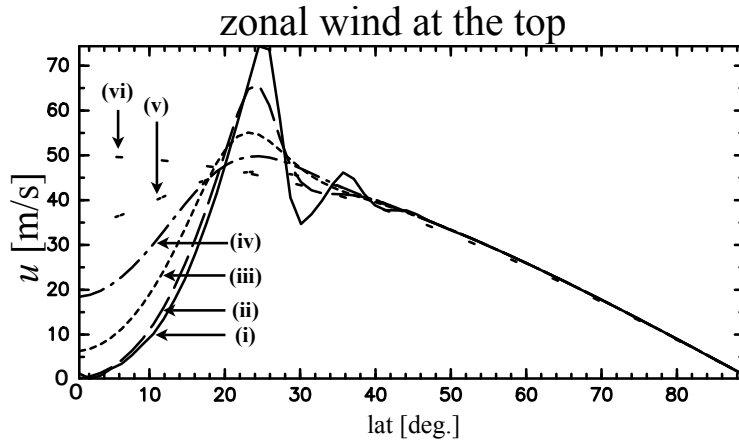


Fig. 6: Meridional profile of zonal winds at the top boundary. Values of the sweep parameters are  $E_H =$  (i)  $3.3 \times 10^{-9}$ , (ii)  $3.3 \times 10^{-6}$ , (iii)  $1.3 \times 10^{-5}$ , (iv)  $3.3 \times 10^{-5}$ , (v)  $1.3 \times 10^{-4}$ , (vi)  $1.3 \times 10^{-1}$ ,  $R_T = 1.2 \times 10^{-1}$ , and  $E_V = 2.1 \times 10^{-4}$ .

## 6. SUMMARY

Axisymmetric steady solutions of planetary atmospheres are investigated numerically with an idealized system: the primitive equations of Boussinesq fluid forced by a Newtonian heating/cooling. Transitions from the Held and Hou (HH hereafter) type Hadley circulation to the super-rotation state driven by the Gierasch mechanism are investigated with a parameter sweep experiment. The dependence of the solution on the external thermal Rossby number ( $R_T$ ), the horizontal Ekman number ( $E_H$ ), and the vertical Ekman number ( $E_V$ ) are explored.

To analyze the transition dynamically, two indices are introduced: a measure of the intensity of super-rotation ( $S$ ) and a measure of rigid rotation ( $Rg$ ). Assuming geostrophic balance and cyclostrophic balance, we can estimate the relationship between  $S$  and  $R_T$  as  $S \sim R_T$  for  $R_T \leq 1$  and  $S \sim \sqrt{R_T}$  for  $R_T > 1$ , respectively. This is a good estimate when  $E_H$  is large enough ( $\sim 10^{-1}$ ) as shown in Fig.4. The value of  $Rg$  increases largely in a certain range of  $E_H$  which depends on  $R_T$  and  $E_V$ , then becomes close to unity (Fig.5), showing that the transition of circulation pattern takes place from the HH type to rigid rotation. An approximate position of this transition is estimated as  $E_H \sim E_V S$ , using the HH theory as shown by arrows in Fig.5.

In this study, we focused on the stable steady solutions obtained by time integrations from a single initial condition. Matsuda (1980, M80 hereafter) drew the famous regime diagrams of dynamical balance types for three cases: (i) infinite horizontal diffusion in zonal momentum equation (Fig.2 of M80), (ii) finitely large horizontal diffusion in zonal momentum equation (Fig.9 of M80), (iii) finitely large horizontal diffusion in zonal and latitudinal momentum equations and thermodynamic equation (Fig.10 of M80). Now, our study has horizontal diffusion in both zonal and latitudinal momentum equations but not in thermodynamic equation, so the situation is not identical to (i), (ii), or (iii). However, in the latitudinal momentum equation, the horizontal diffusion term is much less than other dominant terms, at least, in our parameter range. Therefore, our study may correspond to Fig.9 of M80, so that there is a possibility for the existence of multiple equilibrium solutions in our parameter range. As a next step, it is interesting to explore the multiple equilibrium solutions including unstable steady ones.

## ACKNOWLEDGMENTS

We thank Professor Shin-ichi Takehiro for useful comments. ISPACK-0.71<sup>12</sup>) and LAPACK (<http://www.netlib.org/lapack/>) were used for numerical experiments and analyses. Figures were produced by GFD-DENNOU Libraries (<http://www.gfd-dennou.org/index.html.en>) and MjoGraph (<http://www.oc.hialab.dnj.ynu.ac.jp/mjograph/index.html>).

## REFERENCES

- 1) Schneider, E. K., “Axially symmetric steady-state models of the basic state for instability and climate studies. II. Nonlinear calculations”, *J. Atmos. Sci.* 34 (1977), pp.280-296.
- 2) Held, I. M., and A. Y. Hou, “Nonlinear axially symmetric circulations in a nearly inviscid atmosphere”, *J. Atmos. Sci.* 37 (1980), pp.515-533.
- 3) Vallis, G. K. : Atmospheric and Oceanic Fluid Dynamics, 1st ed. (Cambridge University Press, 2006), p.745.
- 4) Lindzen, R. S. : Dynamics in Atmospheric Physics, 1st ed. (Cambridge University Press, 1990), p.310.
- 5) James, I. N. : Introduction to Circulating Atmospheres, 1st ed. (Cambridge University Press, 1994), p.422.

- 6) Satoh, M., "Hadley circulation in radiative-convective equilibrium in an axially symmetric atmosphere", *J. Atmos. Sci.* 51 (1994), pp.1947-1968.
- 7) Williams, G. P., "Jet sets", *J. Meteor. Soc. Japan* 81 (2003), pp.439-476.
- 8) Gierasch, P., "Meridional circulation and the maintenance of the Venus atmospheric rotation", *J. Atmos. Sci.* 32 (1975), pp.1038-1044.
- 9) Matsuda, Y., "Dynamics of the four-day circulation in the Venus atmosphere", *J. Meteor. Soc. Japan* 58 (1980), pp.443-470.
- 10) Matsuda, Y., "A further study of dynamics of the four-day circulation in the Venus atmosphere", *J. Meteor. Soc. Japan* 60 (1982), pp.245-254.
- 11) Becker, E., "Symmetric stress tensor formulation of horizontal momentum diffusion in global models of atmospheric circulation", *J. Atmos. Sci.* 58 (2001), pp.269-282.
- 12) Ishioka, K., "ispack-71", <http://www.gfd-dennou.org/arch/ispack/>, GFD Dennou Club. (2005)